Journal of Nuclear Medicine, published on July 14, 2016 as doi:10.2967/jnumed.115.165498

Absolute Myocardial Blood Flow and Flow Reserve Assessed by Gated SPECT with Cadmium-Zinc-Telluride Detectors Using 99mTc-Tetrofosmin: Head to Head Comparison with 13N-Ammonia PET

Brief title: Absolute myocardial blood flow by SPECT

Rene Nkoulou, MD*, Tobias A Fuchs, MD*, Aju P Pazhenkottil, MD, Silke M Kuest, MD, Jelena R Ghadri, MD, Julia Stehli, MD, Michael Fiechter, MD, Bernhard A Herzog, MD, Oliver Gaemperli, MD, Ronny R Buechel, MD, Philipp A Kaufmann†

*Rene Nkoulou and Tobias A Fuchs share first authorship

† Ronny R Buechel and Philipp A Kaufmann share last authorship

Department of Nuclear Medicine, Cardiac Imaging, University Hospital Zurich and University of Zurich, Switzerland

Total word count: 4836

Abtract word count: 248

First Author:

Rene Nkoulou, MD
Dept. of Nuclear Medicine
University Hospital Zurich
Ramistr. 100 (NUK D 6) CH-8091 Zurich, Switzerland

Tel. +41-44-255 1111
Fax. +41-44-255 4428

Corresponding author:

Philipp A Kaufmann, MD, FESC, FSCCT
Professor & Chair Dept. of Nuclear Medicine
Director of Cardiac Imaging (CT, MRI, SPECT, PET, Hybrid)
University Hospital Zurich
Ramistr. 100 (NUK D 6) CH-8091 Zurich, Switzerland

Tel. +41-44-255 4196
Fax. +41-44-255 4428
mail pak@usz.ch

Institutional research contract with GE Healthcare

ABSTRACT

Recent advances in SPECT technology including cadmium zinc telluride (CZT) semi-conductor detector material may pave the way for absolute myocardial blood flow (MBF) measurements by SPECT. The aim of the present study was to compare K1 uptake rate constants as surrogates of absolute MBF and myocardial flow reserve index (MFRi) in humans as assessed with a CZT SPECT camera versus positron emission tomography (PET).

Methods: Absolute MBF was assessed in 28 consecutive patients undergoing adenosine stress/rest myocardial perfusion imaging (MPI) by 99mTc-tetrofosmin CZT SPECT and ^{13}N-ammonia PET and MFR was calculated as ratio of hyperaemic over resting MBF. Results from both MPI methods were compared and correlation coefficients were calculated. Diagnostic accuracy of CZT MFRi to predict an abnormal MFR defined as PET MFR<2 was assessed using a receiver operator characteristic curve (ROC).

Results: Median MBF at rest was comparable between CZT and PET (0.89 [0.77-1.00] ml/g/min vs. 0.92 [0.78-1.06] ml/g/min; p=ns) while it was significantly lower at stress in CZT vs PET (1.11 [1.00-1.26] ml/g/min vs 2.06 [1.48-2.56] ml/g/min; p<0.001). This resulted in median MFRi values of 1.32 [1.13-1.52] by CZT and 2.36 [1.57-2.71] by PET (p<0.001). ROC revealed a cut-off for CZT MFRi at 1.26 to predict an abnormal PET MFR yielding an accuracy of 75%.

Conclusion: Estimation of absolute MBFi values by CZT SPECT MPI with 99mTc-tetrofosmin is technically feasible, although hyperemic values are significantly lower than from PET with 13N-ammonia resulting in a substantial underestimation of MFR. Nevertheless, CZT MFRi may confer diagnostic value.

Keywords: myocardial flow reserve (MFR), myocardial blood flow (MBF), cadmium zinc telluride (CZT) SPECT, 13N-Ammonia PET

INTRODUCTION

The definition of coronary artery disease (CAD) was originally based on the presence of anatomic luminal narrowing greater than 50%. Over the past decades, however, many advances in imaging techniques have enhanced our pathophysiologic understanding of CAD. It has been recognized that many factors beyond luminal narrowing may determine whether or not an anatomical coronary lesion induces ischemia. As this cannot be comprehensively addressed by coronary angiography alone, nuclear myocardial perfusion imaging (MPI) has been well established as a tool for providing proof of ischemia. This is mandatory for prognostically relevant target lesion revascularization in chronic stable CAD. As revascularization of a non-flow limiting coronary stenosis is not beneficial to the patient, neither from a prognostic nor from a symptomatic point of view nuclear MPI has been suggested as a gatekeeper for invasive coronary angiography (*1-3*). MPI studies with positron emission tomography (PET) have demonstrated that absolute myocardial blood flow (MBF) and flow reserve (MFR) provide incremental diagnostic (*4*) and prognostic (*5*) information over relative perfusion alone. Quantitative assessment of MBF is difficult with standard SPECT where detectors need to rotate around the patient and where unfavorable properties of the currently available flow tracers hamper accurate MBF quantification due to non-linear extraction fraction with roll-off at higher flow values. The recent advances in SPECT technology including semi-conductor detector material (cadmium zinc telluride; CZT) allow acquisition in a non-rotating mode and therefore acquisition of time-activity curves. This may enable absolute MBF and MFR estimation by single photon computed tomography (SPECT) as recently shown in experimental animal models (*6*) which may pave the way for its implementation in clinical routine (*7*). More knowledge on the impact of the tracer properties on the values obtained from quantification is crucial.

The aim of the present study was a head-to-head comparison in humans of indexes of absolute MBF and MFR as assessed with 99mTc-tetrofosmin on a CZT SPECT camera versus MBF and MFR measured with 13N-ammonia on a PET scanner.

MATERIALS AND METHODS

Patient Population

Thirty-two consecutive patients referred to nuclear MPI with either CZT SPECT or PET for clinical evaluation were enrolled. For study purposes the patients underwent a second MPI with the respective other modality to obtain a pair of SPECT and PET MPI for each patient. In patients without any therapeutic intervention (i.e. no revascularization and no change in medication) a time interval of 2 weeks was accepted. In patients with no therapeutic intervention and chronic stable conditions a maximal time interval of 12 weeks was accepted. The sequence was SPECT first in 25 and PET first in 7 patients. The local ethics committee approved this study and all subjects signed a written informed consent.

13N-Ammonia PET

The PET MPI scan was acquired during pharmacologic stress with an adenosine protocol at a standard rate (0.14 mg/kg/min) over 6 minutes and at rest according to clinical standards (*4,8*). For the stress acquisition 13N-ammonia (1053 ± 110 MBq) was injected 3 minutes into pharmacologic stress into a peripheral vein. Acquisition was repeated at rest (1203 ± 148 MBq) 50 minutes after completion of the stress scan to allow for isotope decay. Images were acquired during 19 minutes in list-mode on a PET/CT scanner (Discovery ST/RX and Discovery VCT, both GE Healthcare, Milwaukee, WI, USA). Images were reconstructed using a matrix of 128*128 and filtered back projection into dynamic series encompassing the first 4 minutes (9x 10-s, 6x 15-s, 3x 20-s) for absolute MBF quantification and into a static series (15 remaining minutes) for assessment of relative perfusion abnormalities. A low-dose CT transmission scan was used for attenuation correction (*9*).

99mTc-Tetrofosmin CZT SPECT

The CZT MPI scan was acquired on a hybrid SPECT/CT scanner (DNM 570c; GE Healthcare, Milwaukee, WI, USA) using the 1-d stress/rest protocol identical to the described protocol above. The SPECT part is a gamma camera with multi-pinhole collimation and 19 non rotating pixelated CZT detector modules positioned around the patient`s chest with full heart coverage (*10*). Due care was taken to assure that patients were positioned in the middle of the field of view and this was confirmed for each patient after the scan. A low dose CT attenuation scan was acquired using the CT component of the same scanner (*11*). For the stress acquisition 99mTc-tetrofosmin (330±33 MBq) was injected 3 minutes into pharmacologic stress into a peripheral vein. Images were acquired in list-mode over 10 minutes starting immediately (a few seconds) before tracer injection. Five minutes after completion of the first scan a second tracer injection with 3 fold higher dose was administrated according to current guidelines and the same acquisition protocol was applied (*8*). For logistic reasons, in 5 patients a rest/stress sequence was used for CZT scanning. Dynamic series including the first 4 minutes (6 x 10s, 6 x 30s) were generated using a dedicated commercially available software package (Myovation for Alcyone; GE Healthcare, Milwaukee, WI, USA) and reconstructed after attenuation correction using a maximum penalized likelihood iterative reconstruction (40 and 50 iterations applied for the stress and rest dataset, respectively) without scatter correction. A Butterworth post processing filter with cut-off frequency 0.37 cycle/cm and order 7 was equally applied (*10*).

Absolute Myocardial Blood Flow Quantification

The MBF values for 13N-ammonia PET (PET MBF) as well as the MBFi values for 99mTc-tetrofosmin CZT SPECT (CZT MBFi) were estimated using the commercially available PMOD software package (version 3.1, PMOD Technologies Ltd, Zurich, Switzerland) developed and validated at our institution (*12,13*). Regions of interest in the right ventricle cavity, left ventricle cavity, and covering the left ventricular myocardium were automatically generated and minimally modified as necessary by an experienced reader to best match cardiac anatomy and

avoid contamination from extracardiac activity. A one-tissue compartment model described by De Grado et al. was used for tracer kinetic modelling inferring a myocardium tissue density of 1.04 g/ml (*14,15*). Global MBF values were determined after fitting the tissue activity curves of the myocardial as well as right ventricular and left ventricular values (*16*). No specific correction of the quantification process was performed despite the higher residual activity during the second half of CZT study. Furthermore, no correction of the quantification model was applied despite differences in the extraction fraction and metabolites present for 99mTc-tetrofosmin compared to ammonia. Therefore, the MBF values obtained during the CZT study are rather indexes of the flow (MBFi) at rest and stress and their stress/rest ratio is the MFR index (MFRi). An image illustration during dynamic acquisition with CZT is displayed in Figure 1. For reason of quality assurance segments with CZT flow values > 4 ml/g/min or with > 50% difference compared to adjacent segments were qualified as inconceivable values and were therefore discarded. This seemed appropriate in order to account for the tendency to greater contamination from extra cardiac activity and less favorable tracer distribution in addition to lower spatial resolution of CZT compared to the PET. Similarly, patients with global resting MBF PET values > 2 ml/min/g were excluded from further analysis as such values were classified as outliers (4 standard deviations above the reported mean values) according to a large body of evidence (*10*). Global MFR (PET) and MFRi (CZT) were calculated as the ratio of global MBF and MBFi at stress over rest values. Figure 2 depicts representative images of a patient's 99mTc-tetrofosmin CZT SPECT and 13N-ammonia PET studies at stress and rest.

Statistical Analysis

The continuous values were summarized as mean ± standard deviation and parametric values as percentage or median and interquartile range as appropriate. Shapiro Wilk test was used to test for normal distribution. Results from both MPI methods were compared using Wilcoxon signed rank test and spearman correlation coefficient was calculated. A receiver

operator characteristics (ROC) analysis was conducted to evaluate the diagnostic accuracy of CZT in the detection of patients with MFR < 2 by PET. All P values < 0.05 were considered statistically significant. SPSS 22.0 (SPSS, Chicago, IL, USA) was used for the statistical analysis.

RESULTS

Four patients were excluded from further analysis according to predefined quality criteria for quantitative PET. The final study population consisted of 28 patients (86% males) with a mean age of 64 ± 10 years and a BMI of 28 ± 6 kg/m^2 (Table 1). Kinetic modeling curves and polar maps at rest and stress for a representative patient are displayed using PET (Figure 3) and CZT (Figure 4).

A total of 952 segments (476 stress and 476 rest) were analyzed in the 28 patients by CZT and PET. According to prespecified quality criteria for CZT measurements a total of 79 segments (8%) had to be excluded (28 stress and 51 rest scans). At rest, median MBFi with CZT was similar to MBF with PET (0.89 [0.77-1.00]ml/g/min vs. 0.92 [0.78-1.06]ml/g/min; p=ns) while CZT MBFi was significantly lower at stress vs PET MBF (1.11 [1.00-1.26] ml/g/min vs. 2.06 [1.48-2.56] ml/g/min; p<0.001). This resulted in median MFRi values of 1.32 [1.13-1.52] by CZT which was significantly lower than the MFR value of 2.36 [1.57-2.71] by PET (p<0.001).

Overall the correlation between CZT MBFi and PET MBF values was ρ = 0.62 (p<0.001), whereas the correlations for MBFi and MBF at rest and stress were ρ = 0.51 (p<0.05) and ρ = 0.30 (p= ns) (Figure 5).

The ROC revealed a cut-off for CZT MFRi at 1.26 to predict an abnormal PET MFR. Using the latter cut-off value, CZT correctly identified 14/18 patients (specificity: 78%) with PET

MFR ≥ 2 and 7/10 (sensitivity: 70%) with PET MFR < 2, yielding an accuracy of 75% (Figure 6). The MBF values at rest and stress in patients with correctly identified and misidentified PET MFR when using CZT is displayed in Table 2.

DISCUSSION

Our study is the first to compare in humans MBF data from dynamic CZT acquisition with data from PET, which is considered the gold standard for quantitative non-invasive MBF assessment (*17*). Our results demonstrate that quantification of dynamic SPECT MPI on modern CZT cameras is technically feasible but without specific correction for the different extraction fraction and metabolism of 99mTc-tetrofosmin underestimates MBF values at high flow conditions. While resting MBFi values from CZT did not differ significantly from PET MBF values, hyperemic MBF values were significantly underestimated by CZT MBFi resulting in underestimation of MFRi values obtained from CZT MBFi quantification. The key finding is that, nevertheless, values of CZT MFRi revealed an accuracy of 75% to assess an abnormal MFR documented by PET.

Previous studies exploring quantification of MBF with dynamic planar scintigraphy in humans (*18-25*) and with dynamic SPECT in experimental animals (*26-28*) have documented the limitations of conventional gamma cameras for the dynamic acquisition of data sets required for MBF quantification. The introduction of CZT cameras without the need of detector rotation has allowed proving the concept of dynamic image acquisition for MBF quantification in a recent animal study using microspheres as standard of reference (*6*). A recent study has confirmed the feasibility and reproducibility of kinetic analysis of myocardial tracer uptake with a CZT device, (*29*) although no standard of reference for perfusion quantification was available.

Our CZT MFRi values are in line with the values reported by Ben-Haim et al (*29*) and are substantially lower than the MFR values estimated by PET. This was mainly driven by the lower MBF values observed by SPECT at high flow conditions, while resting MBF values were highly comparable with PET. This is explained at least in part by the well-known properties of 99mTc-tetrofosmin, namely inferior extraction at high flow rates compared to 13N-ammonia. The superiority of 13N-ammonia of 99mTc-tetrofosmin is not only evidenced by a higher extraction

fraction at resting conditions (80% versus 53%) but also based on the fact that the given extraction fraction remains constant over a much larger range of MBF. This explains why the model for correction of 13N-ammonia MBF values may not provide a satisfying fit for 99mTc-tetrofosmin. Our results are in perfect agreement with the notion (*6*) that contrast between stress and resting flow will be lower for 99mTc-tracers (*23,29*) than typically seen with PET (*17*).

However, in daily clinical practice qualitative SPECT MPI is a well-established tool for diagnostic and prognostic CAD estimation (*30*) indicating that despite the limited contrast of stress vs rest this technique provides powerful discrimination of health and disease in CAD. Given the growing body of evidence underlining the importance of absolute MBF and MFR quantification our findings may have important clinical implications to further emphasize the role of SPECT MPI. In fact, although the MFR values were significantly lower by CZT than those assessed by PET due to the flattening of the curve at hyperemia, the CZT MFRi nevertheless confers a strong discriminatory power (accuracy of 75%) of normal versus abnormal myocardial perfusion. Despite the limited size of the study the strength of these results lies in the fact that each patient served as their own internal control and the cut-off for abnormal perfusion detection was a PET MFR < 2, which is a robust and widely accepted threshold both for diagnostic (*4*) and prognostic CAD assessment (*5,31*). 99mTc-tetrofosmin was used in this study because it constitutes the most commonly used radiotracer used for SPECT MPI in daily clinical routine. However 99mTc-tracers with more favorable tracer kinetics such as found for teboroxime (*32*) may help improving the role of MFR by CZT.

It may be perceived as a potential limitation of the present study that no invasive coronary angiography was performed. However, the aim of the study was the evaluation of quantitative MBF and MFR assessed by CZT SPECT and therefore quantitative PET perfusion seemed the most appropriate standard of reference while an anatomic definition of CAD could only provide dichotomous information on presence and absence of disease. Furthermore, an

anatomic reference would represent a flawed gold standard for quantitative MBF measurements and would require assessment of invasive fractional flow reserve (FFR), which is not feasible for ethical reasons due to its invasive nature in patients with normal findings. Furthermore, we have confined our study to global rather than regional values which may potentially constitute a limitation. However, global MFR reflects CAD beyond the epicardial section of the coronary tree involving microcirculation, including endothelial dysfunction, which has been shown to increase the sensitivity in detecting CAD when global MFR is used as an adjunct to PET MPI. The use of global MFR appears to be most appropriate when the aspect of microcirculatory dysfunction is included, which is often associates with CAD. Furthermore, for reasons of feasibility implementation of global MFR seems preferable over regional MFR because the reproducibility and the repeatability of global MFR is considerably superior to that of regional MFR from PET (*13,33*). This may apply even more for SPECT measurements due to technical issues and count statistics including lower spatial resolution which may affect the apparent perfusion values in a non-homogenous manner, leading to different patterns in the polar plots for PET and SPECT as depicted in Figures 3 and 4. It is also based on biologic variability, as a profound spatial heterogeneity has been observed in regional MBF at rest and in response to vasodilator stress (*34,35*). The anatomic variability of the coronary trees is another source which has been shown to affect the per-segment performance of quantitative MBF measurements. Finally, our study has been performed using an integrated SPECT-CT but without scatter correction and therefore extrapolation to protocols with separate acquisition on standalone CT and CZT SPECT scanners and to protocols using scatter correction should be done with caution.

CONCLUSION

Conclusion: Estimation of absolute MBFi values by CZT SPECT MPI with 99mTc-tetrofosmin is technically feasible, although hyperemic values are significantly lower than from

PET with 13N-ammonia resulting in a substantial underestimation of MFR. Nevertheless, CZT MFRi may confer diagnostic value.

ACKNOWLEDGEMENTS

The study was supported by a grant from the Swiss National Science Foundation to Philipp Antonio Kaufmann. We thank our radiographers Ennio Muller and Edlira Loga for their excellent technical support.

CONFLICT OF INTEREST

Institutional research contract with GE Healthcare.

REFERENCES

1. Windecker S, Kolh P, Alfonso F, et al. 2014 ESC/EACTS guidelines on myocardial revascularization: The task force on myocardial revascularization of the European Society of Cardiology (ESC) and the European Association for Cardio-Thoracic Surgery (EACTS) developed with the special contribution of the European Association of Percutaneous Cardiovascular Interventions (EAPCI). *Eur Heart J.* 2014;35:2541-2619.

2. Herzog BA, Wyss CA, Husmann L, et al. First head-to-head comparison of effective radiation dose from low-dose 64-slice CT with prospective ECG-triggering versus invasive coronary angiography. *Heart.* 2009;95:1656-1661.

3. Hendel RC, Berman DS, Di Carli MF, et al. ACCF/ASNC/ACR/AHA/ASE/SCCT/SCMR/SNM 2009 Appropriate use criteria for cardiac radionuclide imaging: a report of the American College of Cardiology Foundation Appropriate Use Criteria Task Force, the American Society of Nuclear Cardiology, the American College of Radiology, the American Heart Association, the American Society of Echocardiography, the Society of Cardiovascular Computed Tomography, the Society for Cardiovascular Magnetic Resonance, and the Society of Nuclear Medicine. *J Am Coll Cardiol.* 2009;53:2201-2229.

4. Ghadri JR, Fiechter M, Veraguth K, et al. Coronary calcium score as an adjunct to nuclear myocardial perfusion imaging for risk stratification before noncardiac surgery. *Journal of Nuclear Medicine.* 2012;53:1081-1086.

5. Herzog BA, Husmann L, Valenta I, et al. Long-term prognostic value of 13N-ammonia myocardial perfusion positron emission tomography added value of coronary flow reserve. *J Am Coll Cardiol.* 2009;54:150-156.

6. Wells RG, Timmins R, Klein R, et al. Dynamic SPECT measurement of absolute myocardial blood flow in a porcine model. *J Nucl Med.* 2014;55:1685-1691.

7. Bocher M, Blevis IM, Tsukerman L, Shrem Y, Kovalski G, Volokh L. A fast cardiac gamma camera with dynamic SPECT capabilities: design, system validation and future potential. *Eur J Nucl Med Mol Imaging.* 2010;37:1887-1902.

8. Verberne HJ, Acampa W, Anagnostopoulos C, et al. EANM procedural guidelines for radionuclide myocardial perfusion imaging with SPECT and SPECT/CT: 2015 revision. *Eur J Nucl Med Mol Imaging.* 2015;42:1929-1940.

9. Koepfli P, Hany TF, Wyss CA, et al. CT attenuation correction for myocardial perfusion quantification using a PET/CT hybrid scanner. *J Nucl Med.* 2004;45:537-542.

10. Herzog BA, Buechel RR, Katz R, et al. Nuclear myocardial perfusion imaging with a cadmium-zinc-telluride detector technique: optimized protocol for scan time reduction. *J Nucl Med.* 2010;51:46-51.

11. Herzog BA, Buechel RR, Husmann L, et al. Validation of CT attenuation correction for high-speed myocardial perfusion imaging using a novel cadmium-zinc-telluride detector technique. *J Nucl Med.* 2010;51:1539-1544.

12. Siegrist PT, Gaemperli O, Koepfli P, et al. Repeatability of cold pressor test-induced flow increase assessed with H(2)(15)O and PET. *J Nucl Med.* 2006;47:1420-1426.

13. Wyss CA, Koepfli P, Mikolajczyk K, Burger C, von Schulthess GK, Kaufmann PA. Bicycle exercise stress in PET for assessment of coronary flow reserve: repeatability and comparison with adenosine stress. *J Nucl Med.* 2003;44:146-154.

14. DeGrado TR, Hanson MW, Turkington TG, et al. Estimation of myocardial blood flow for longitudinal studies with 13N-labeled ammonia and positron emission tomography. *J Nucl Cardiol.* 1996;3:494-507.

15. Nekolla SG, Reder S, Saraste A, et al. Evaluation of the novel myocardial perfusion positron-emission tomography tracer 18F-BMS-747158-02: comparison to 13N-ammonia and validation with microspheres in a pig model. *Circulation.* 2009;119:2333-2342.

16. Cerqueira MD, Weissman NJ, Dilsizian V, et al. Standardized myocardial segmentation and nomenclature for tomographic imaging of the heart: a statement for healthcare professionals from the Cardiac Imaging Committee of the Council on Clinical Cardiology of the American Heart Association. *Circulation.* 2002;105:539-542.

17. Gould KL, Johnson NP, Bateman TM, et al. Anatomic versus physiologic assessment of coronary artery disease. Role of coronary flow reserve, fractional flow reserve, and positron emission tomography imaging in revascularization decision-making. *J Am Coll Cardiol.* 2013;62:1639-1653.

18. Taki J, Fujino S, Nakajima K, et al. (99m)Tc-sestamibi retention characteristics during pharmacologic hyperemia in human myocardium: comparison with coronary flow reserve measured by Doppler flowire. *J Nucl Med.* 2001;42:1457-1463.

19. Ito Y, Katoh C, Noriyasu K, et al. Estimation of myocardial blood flow and myocardial flow reserve by 99mTc-sestamibi imaging: comparison with the results of [15O]H2O PET. *Eur J Nucl Med Mol Imaging.* 2003;30:281-287.

20. Storto G, Cirillo P, Vicario ML, et al. Estimation of coronary flow reserve by Tc-99m sestamibi imaging in patients with coronary artery disease: comparison with the results of intracoronary Doppler technique. *J Nucl Cardiol.* 2004;11:682-688.

21. Storto G, Soricelli A, Pellegrino T, Petretta M, Cuocolo A. Assessment of the arterial input function for estimation of coronary flow reserve by single photon emission computed tomography: comparison of two different approaches. *Eur J Nucl Med Mol Imaging.* 2009;36:2034-2041.

22. Marini C, Giusti M, Armonino R, et al. Reduced coronary flow reserve in patients with primary hyperparathyroidism: a study by G-SPECT myocardial perfusion imaging. *Eur J Nucl Med Mol Imaging.* 2010;37:2256-2263.

23. Daniele S, Nappi C, Acampa W, et al. Incremental prognostic value of coronary flow reserve assessed with single-photon emission computed tomography. *J Nucl Cardiol.* 2011;18:612-619.

24. Alhassen F, Nguyen N, Bains S, et al. Myocardial blood flow measurement with a conventional dual-head SPECT/CT with spatiotemporal iterative reconstructions - a clinical feasibility study. *Am J Nucl Med Mol Imaging.* 2013;4:53-59.

25. Hsu B, Chen FC, Wu TC, et al. Quantitation of myocardial blood flow and myocardial flow reserve with 99mTc-sestamibi dynamic SPECT/CT to enhance detection of coronary artery disease. *Eur J Nucl Med Mol Imaging.* 2014;41:2294-2306.

26. Iida H, Eberl S. Quantitative assessment of regional myocardial blood flow with thallium-201 and SPECT. *J Nucl Cardiol.* 1998;5:313-331.

27. Christian TF, Peters K, Keck B, Allen J, Owens T, Borah B. Gated SPECT imaging to detect changes in myocardial blood flow during progressive coronary occlusion. *Int J Cardiovasc Imaging.* 2008;24:269-276.

28. Iida H, Eberl S, Kim KM, et al. Absolute quantitation of myocardial blood flow with (201)Tl and dynamic SPECT in canine: optimisation and validation of kinetic modelling. *Eur J Nucl Med Mol Imaging.* 2008;35:896-905.

29. Ben-Haim S, Murthy VL, Breault C, et al. Quantification of myocardial perfusion reserve using dynamic SPECT imaging in humans: a feasibility study. *J Nucl Med.* 2013;54:873-879.

30. Doukky R, Hayes K, Frogge N, et al. Impact of appropriate use on the prognostic value of single-photon emission computed tomography myocardial perfusion imaging. *Circulation.* 2013;128:1634-1643.

31. Ziadi MC, Dekemp RA, Williams KA, et al. Impaired myocardial flow reserve on rubidium-82 positron emission tomography imaging predicts adverse outcomes in patients assessed for myocardial ischemia. *J Am Coll Cardiol.* 2011;58:740-748.

32. Di Bella EV, Ross SG, Kadrmas DJ, et al. Compartmental modeling of technetium-99m-labeled teboroxime with dynamic single-photon emission computed tomography: comparison with static thallium-201 in a canine model. *Invest Radiol.* 2001;36:178-185.

33. Kaufmann PA, Gnecchi-Ruscone T, Yap JT, Rimoldi O, Camici PG. Assessment of the reproducibility of baseline and hyperemic myocardial blood flow measurements with 15O-labeled water and PET. *J Nucl Med.* 1999;40:1848-1856.

34. Austin RE, Jr., Aldea GS, Coggins DL, Flynn AE, Hoffman JI. Profound spatial heterogeneity of coronary reserve. Discordance between patterns of resting and maximal myocardial blood flow. *Circ Res.* 1990;67:319-331.

35. Chareonthaitawee P, Kaufmann PA, Rimoldi O, Camici PG. Heterogeneity of resting and hyperemic myocardial blood flow in healthy humans. *Cardiovasc Res.* 2001;50:151-161.

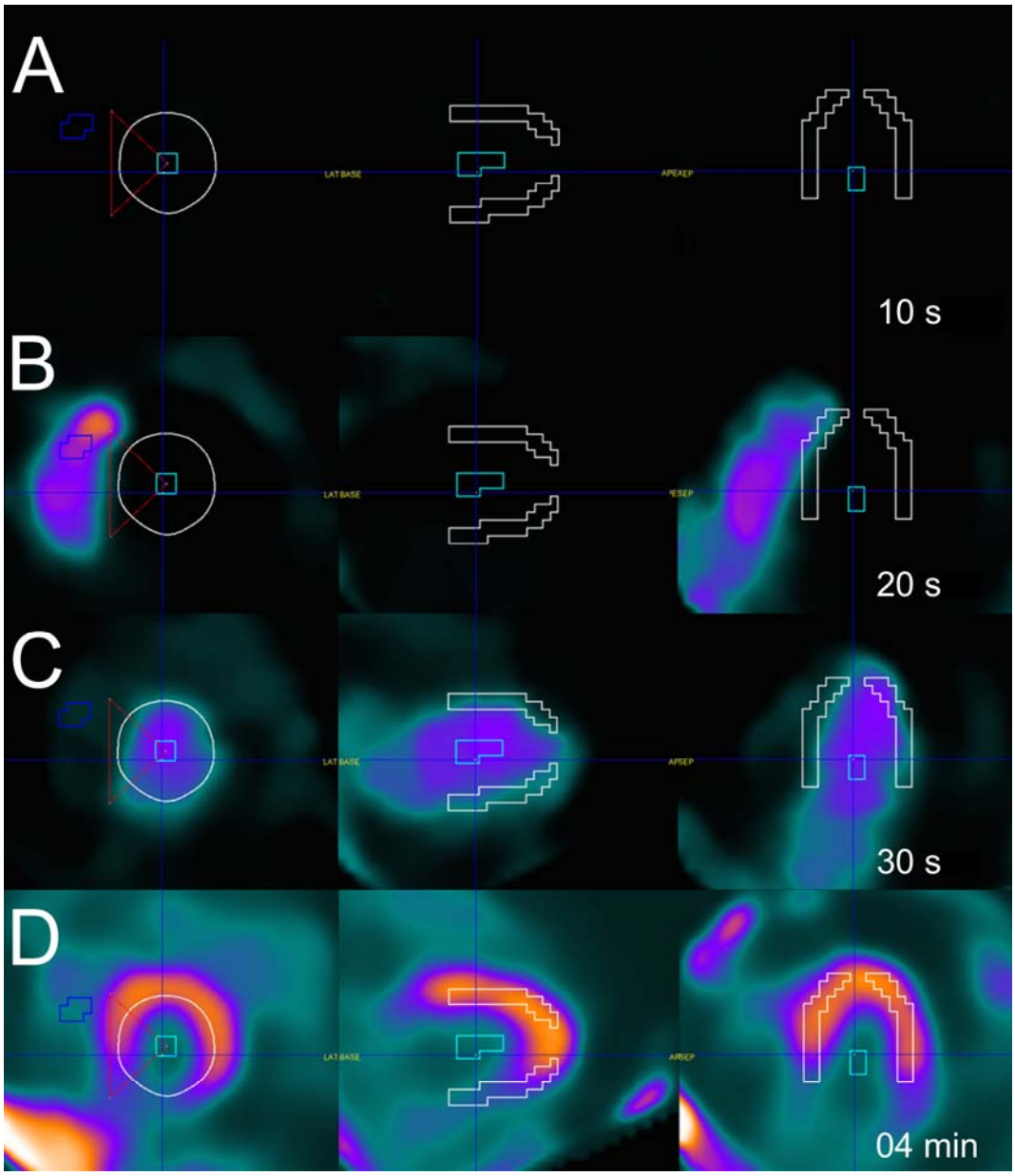

Figure 1 Dynamic cadmium zinc telluride SPECT imaging during adenosine stress. Short axis (left column), vertical (middle column) and horizontal long axis (right column) frames with the region of interest drawn in the right and left ventricle and the left ventricular myocardium (A). Dynamic acquisition sequentially illustrates the right ventricular inflow (B), the left ventricular inflow (C) and the myocardial perfusion (D).

White ROI: myocardium; light blue ROI: left ventricular cavity; dark blue ROI: right ventricular cavity; red triangle: delineation of upper and lower interventricular junction and the middle of left ventricular cavity.

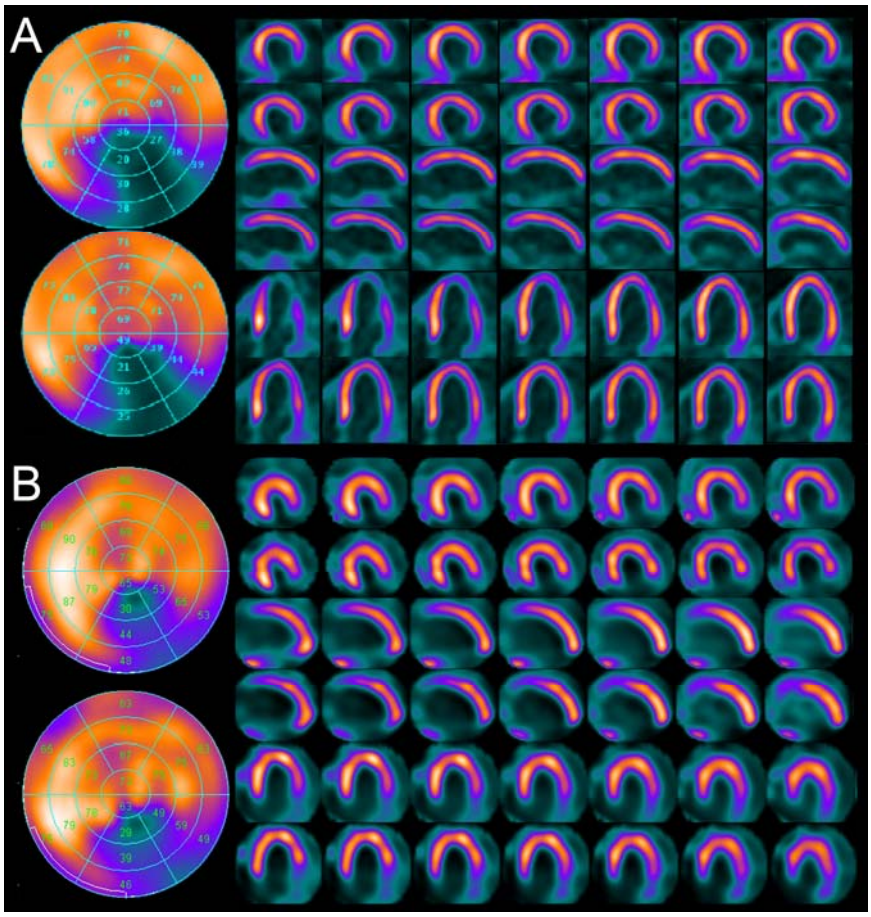

Figure 2 Static 99mTc-tetrofosmin cadmium zinc telluride SPECT (A) and 13N-ammonia PET (B) images acquired during stress (top rows) and at rest (bottom rows). Images were obtained from the same patient as in Figure 1.

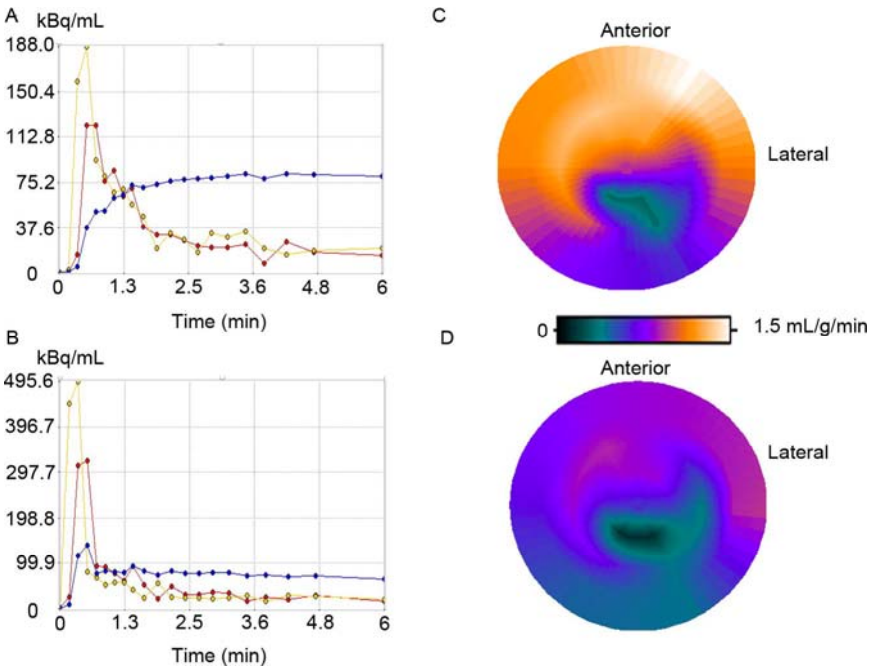

Figure 3 Fit curves and polar map of a representative patient when using PET. Upper panel: fit curves (A) and polar map (C) at stress. Lower panel: fit curves (B) and polar map (D) at rest. Yellow curves: right ventricule; red curves: left ventricule; blue curves: myocardium.

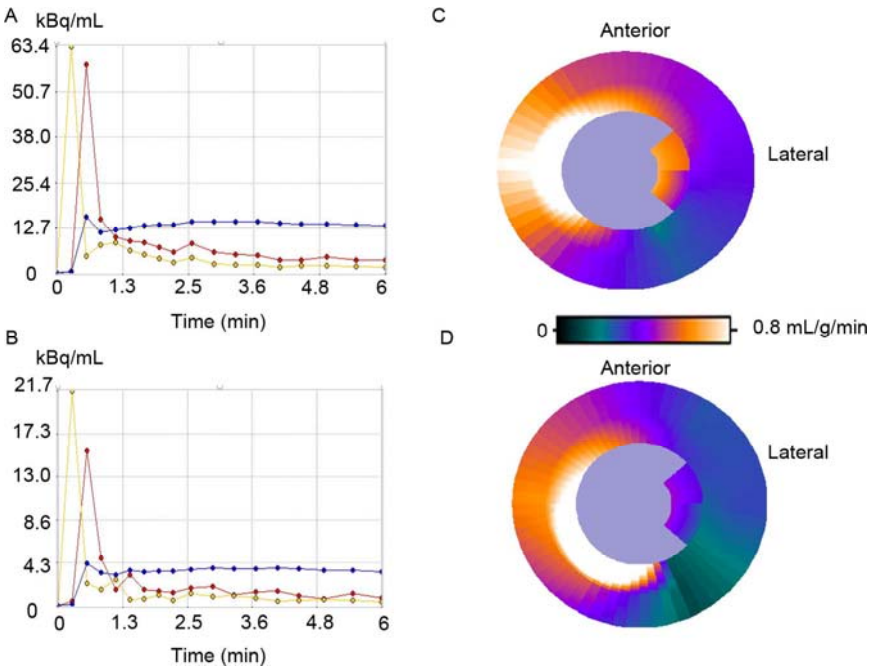

Figure 4 Fit curves and polar map of the same patient when using CZT. Upper panel: fit curves (A) and polar map (C) at stress. Lower panel: fit curves (B) and polar map (D) at rest.Yellow curves: right ventricule; red curves: left ventricule; blue curves: myocardium. The apical intense myocardial activity could be due to lower spatial resolution and myocardial ROI contamination by LV activity.

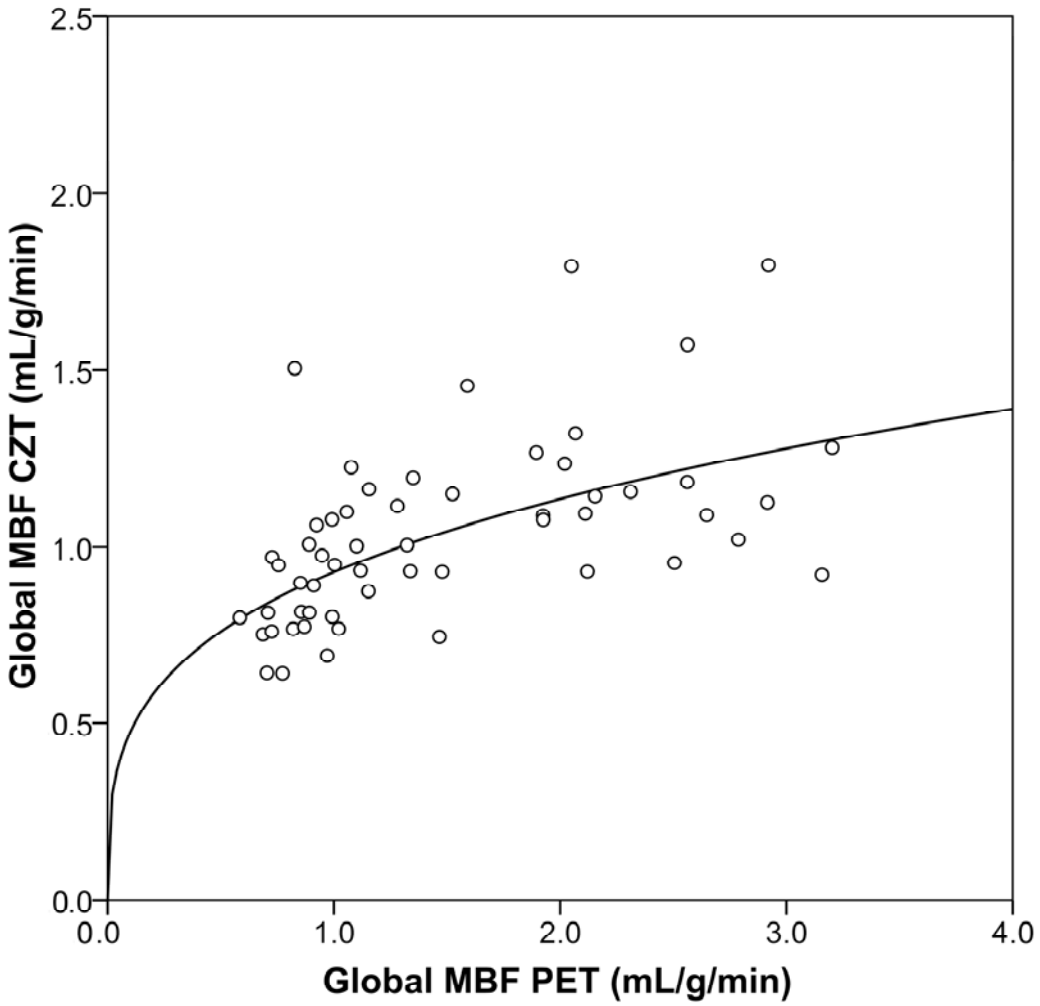

Figure 5 Head-to-head comparison of myocardial blood flow values obtained from cadmium zinc telluride (CZT) SPECT versus PET which served as standard of reference. The flattening of the curve at values above 1 ml/g/min indicates an underestimation by CZT SPECT particularly under high flow conditions.

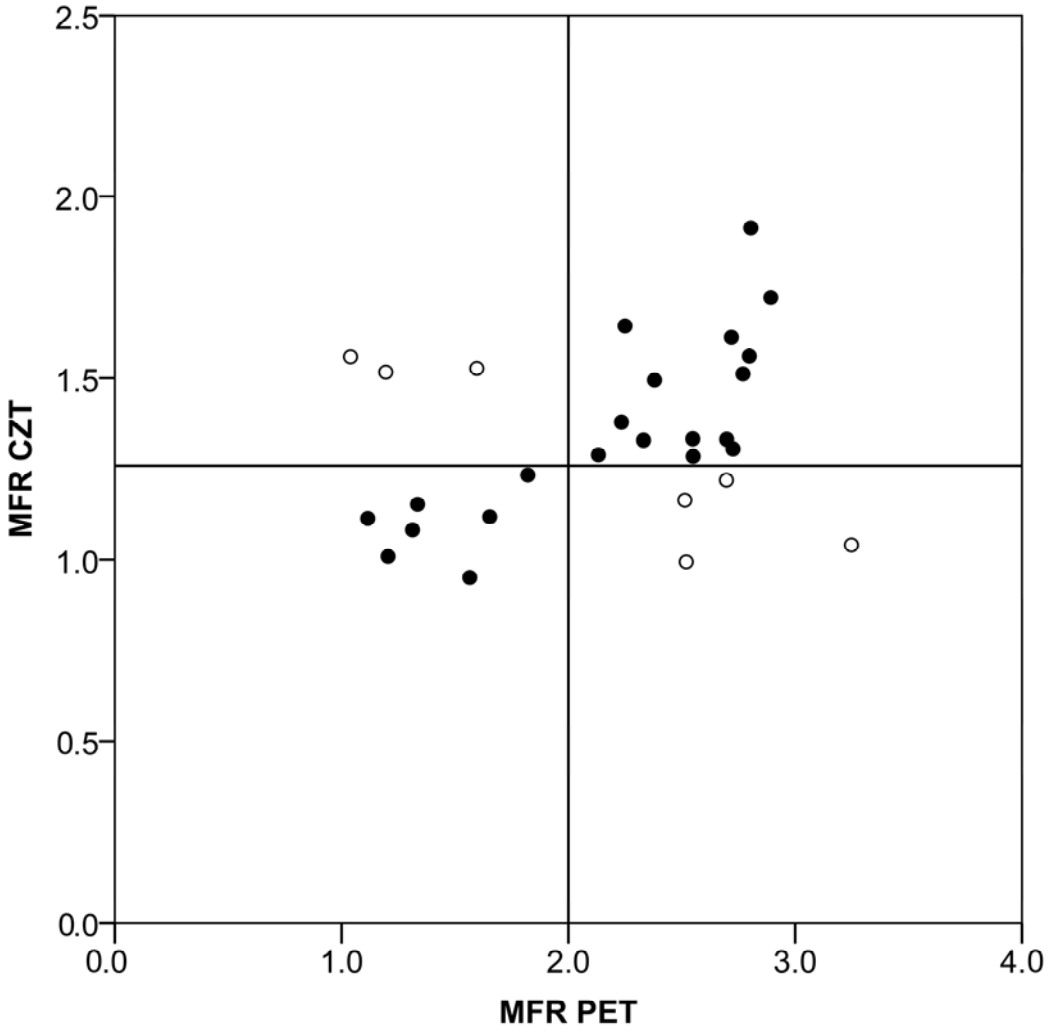

Figure 6 Using a cut-off value of 1.26 (as identified by ROC) for myocardial flow reserve (MFR) index cadmium zinc telluride (CZT) correctly identified (black circles) 14/18 patients (specificity: 78%) with PET myocardial flow reserve ≥ 2 and 7/10 (sensitivity: 70%) with PET MFR < 2. This results in an accuracy of 75% for CZT MFR index.

Table 1 Patient baseline characteristics (n = 28)

Clinical symptoms, n (%)	
Dyspnea	10 (35)
Typical chest pain	7 (25)
Atypical chest pain	9 (32)
Asymptomatic	6 (21)
Cardiovascular risk factors, n (%)	
Smoking	4 (14)
Diabetes	9 (32)
Arterial hypertension	17 (61)
Dyslipidemia	18 (64)
Positive family history	13 (46)

Values are given as absolute numbers and percentage (in brackets)

Table 2 Myocardial blood flow values at rest and stress in patients with correctly identified and misidentified PET myocardial flow rate index when using SPECT CZT.

PET MFR	CZT MFR	n	PET MBF stress	PET MBF rest	CZT MBFi stress	CZT MBFi rest
high	high	14	2.32 ± 0.45	0.91 ± 0.17	1.20 ± 0.23	0.87 ± 0.15
high	low	4	2.39 ± 0.78	0.85 ± 0.22	1.14 ± 0.45	1.03 ± 0.32
low	low	7	1.57 ± 0.65	1.06 ± 0.27	1.04 ± 0.14	0.96 ± 0.17
low	high	3	1.19 ± 0.43	0.90 ± 0.17	1.18 ± 0.17	0.82 ± 0.22

High PET MFR: myocardial flow rate ≥ 2 as assessed by PET (13N-ammonia); Low PET MFR: myocardial flow rate < 2 as assessed by PET; High CZT MFRi: myocardial flow rate ≥ 1.26 as assessed by SPECT CZT (99mTc-tetrofosmin); Low CZT MFRi: myocardial flow rate < 1.26 as assessed by SPECT CZT. Values given are ml/g/min ± standard deviation.